

A new family of strain tensors based on the hyperbolic sine function

Daniel Henrique Nunes Peixoto^a , Marcelo Greco^{a*} , Daniel Boy Vasconcellos^a 

^aUniversidade Federal de Minas Gerais – UFMG, Programa de Pós-Graduação em Engenharia de Estruturas, Belo Horizonte, MG, Brasil.
Email: danielh_peixoto@hotmail.com, mgreco@dees.ufmg.br, danielboyvasconcellos@gmail.com

*Corresponding author

<https://doi.org/10.1590/1679-78257883>

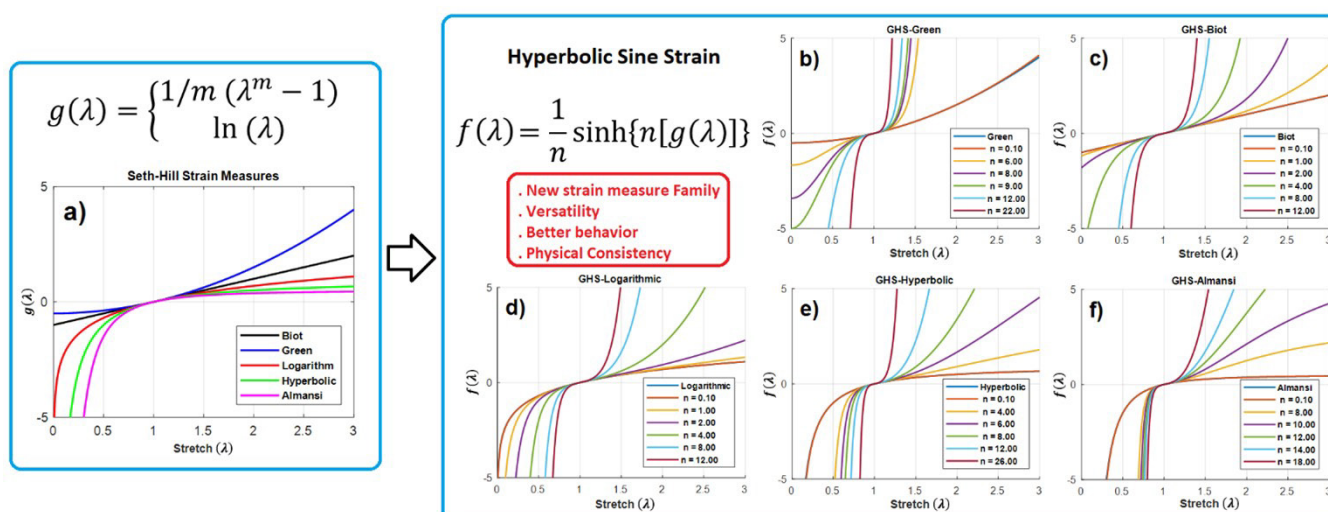
Abstract

This work introduces a new family of strain tensors based on the hyperbolic sine function: The Generalized Hyperbolic Sine (GHS). This family is obtained by using any given strain measure as an argument in a normalized hyperbolic sine function. Particularly, this paper adopts the Seth-Hill family as an argument and shows how some drawbacks of the classical strain measures can be overcome by means of the proposed strain family. A broad analytical study of pure deformation modes (simple axial extension, equi-biaxial loading and simple shear) is presented to show the behavior of the proposed strain family and investigate the physical coherence of their responses. Obtained results are promising as the GHS family proved itself capable of enhancing the physical behavior of the Seth-Hill strain measures and providing versatility with the addition of just one material constant with clear physical meaning. Materials investigated in the article are isotropic and homogeneous. The proposed Hookean-type hyperelastic models can be applied for both incompressible and compressible materials without additional strain energy density function changes.

Keywords

strain measures, hyperbolic sine, hyperelasticity, large strains

Graphical Abstract



Received: November 02, 2023. In revised form: January 08, 2024. Accepted: January 16, 2024. Available online: January 19, 2024

<https://doi.org/10.1590/1679-78257883>



Latin American Journal of Solids and Structures. ISSN 1679-7825. Copyright © 2024. This is an Open Access article distributed under the terms of the [Creative Commons Attribution License](https://creativecommons.org/licenses/by/4.0/), which permits unrestricted use, distribution, and reproduction in any medium, provided the original work is properly cited.

List of Main Symbols

λ, λ_i : stretching; m : integer constant; n : material parameter ($n \in \mathbb{R}^*$); \mathbf{U} : right stretch tensor; α_i : eigenvectors of \mathbf{U} ; $f(\lambda)$: strain function; $\mathbf{\epsilon}^f$: strain tensor associated with $f(\lambda)$; $\boldsymbol{\sigma}^f$: work-conjugated stress with $\mathbf{\epsilon}^f$; $\bar{\sigma}_i^f$: components of $\boldsymbol{\sigma}^f$ in the $\{\alpha_i\}$ basis; \mathbf{F} : deformation gradient; $\boldsymbol{\sigma}^C$: Cauchy stress tensor; \mathbf{P} : first Piola-Kirchhoff stress tensor; E : Young's modulus; ν : Poisson's ratio; z : auxiliary variable; γ : shear parameter; Λ, μ : Lamé parameters.

List of abbreviations

GHS: generalized hyperbolic sine; SAE: simple axial extension; EB-L: equi-biaxial loading; SS: simple shear

1 INTRODUCTION

The justification for the presentation of a new family of strain measures and the study of the classical ones must be made considering that there is no universal hyperelastic model suitable for all types of materials. Considering the vast number of materials used in engineering, a large number of works dedicated to solving this problem is understandable.

Even when working with the same material, finding a universal model is very difficult and different hyperelastic models can provide a better fit with the experimental data depending on the shape of the analyzed structural component, the deformation modes involved, the boundary conditions and the loads applied.

Recently, several interesting works are dedicated to improving hyperelastic modeling. Stumpf & Marczak (2021) presented a new strain energy density satisfying both the Baker-Ericksen inequalities and the positive-definiteness of the tangent operator. Melly et al. (2022) proposed a phenomenological constitutive model for hyperelastic materials that takes the logarithmic form for the second stretching invariant term, based on a polynomial model used in the hyperelasticity theory. Moreover, authors stated that the incompressibility assumption leads to simplified model equations without affecting the accuracy of the hyperelastic models. Kossa et al. (2023) studied the behavior of the compressible, isotropic, neo-Hookean hyperelastic model. To represent compressibility the authors used the standard procedure of using the additive decomposition of the strain energy density function into deviatoric and volumetric parts, however, in compression non-unique solutions were observed and numerical snap-back responses were obtained for some Poisson ratio values. Kang et al. (2023) developed a new form of the multi-axial elastic potential with two invariants of the Logarithmic (Hencky) strain, as an attempt to bypass coupling complexities involved in parameter identification, authors used decoupled independent parameters so data sets for multiple benchmark modes can be separately matched with independent single-variable functions.

Worth mentioning that neural networks have played a highlighted role in constitutive modelling. Park et al. (2023) used these concepts to predict stress-strain curves. The authors optimized dust covers obtaining a reduced maximum equivalent von Mises stress up to 18%. Further, embedding many terms such as polynomial, exponential and logarithmic, Peirclinck et al. (2024) used neural networks to generate 4096 constitutive models. The universal subroutine created by the authors was applied in realistic finite element simulations of the human brain for different head impacts. Firouzi & Amabili (2024) developed formulas for the phenomenological behavior of the biological tissues growth, both incompressible and compressible neo-Hookean models were used. There are also recent relevant works that address the description of the mechanical behavior of soft biological tissues and biomaterials through new hyperelastic models, as an example one can mention the work of Saucedo-Mora et al. (2021), which presents a new hyperelastic model to represent the mechanical behavior of the brain.

In addition to the difficulty of obtaining a universal constitutive model, it should be noted that the fitting of data used in finite element analysis of experimental tests is not an easy task and several difficulties may arise during the procedure, as can be seen in Cao et al. (2017) and Mansouri et al. (2017). For a simple uniaxial test, it is relatively easy to combine curves, but the same is not true for more complex deformation modes.

Therefore, it seems reasonable to think that the use of alternative strain measures, as well as the creation of new strain families, may help in the hyperelastic modeling process. This is because a simple way to generate hyperelastic models is the use of Hookean-type models, presented by Hill (1979), in which the chosen strain measure and its conjugate stress pair are inserted in the context of Hooke's law. This is an approach that reliably leads to the creation of models of hyperelastic materials (Korobeynikov, 2019). The direct generalization of the classical Hooke's law for finite strains, characterized simply by the two elastic Lamé constants evaluated in the infinitesimal strain, is attractive and desirable for purposes of calculations and practical applications for simplicity (Xiao & Chen, 2002). The Hookean-type constitutive models inherit their characteristics from the strain measures that give rise to them. However, it is important to emphasize that even more elaborate models, which use material invariants and constants in the construction of energy density

functions, the tensors to which the invariants belong, and the choice of which strain/stress measure to be used is not irrelevant.

In fact, one of the approaches to universally model hyperelastic materials is using energy density functions represented by large and complex mathematical expressions, composed of several material constants that are calibrated through experimental tests data (Data-Driven approach or Data Driven Modeling). However, in practice, constitutive models with fewer terms and material constants are preferable, even if the correspondence with the experimental data is not the best (Mihai & Goriely, 2017), on the premise that such model consistently represents the behavior of the material qualitatively. Still taking this premise into account, Chagnon et al. (2015) explain that models that use simple functions, with fewer material constants and invariants, generally achieve better results, as they are less likely to create non-physical responses. In the field of biomechanics involving human tissues, for example, where it is more difficult to perform experimental tests and the materials studied have a complex nature and behavior, the current struggle seems to be obtaining good qualitative representation of the material behavior at large strains, as an exact representation still is a distant goal.

The creation and the study of different strain measures are ancient and have been around for centuries. The Almansi (Karni), Hyperbolic (Swanger), Logarithmic (Hencky), Biot and Green measures are usually called classical strain measures. Seth (1961) and later Hill (1968) created the perception that the classical strain measures could be considered as members of a single family, thus creating the so-called Seth-Hill family of strain measures. Korobeynikov (2019) has subdivided the Seth-Hill family into the one-parameter Doyle–Ericksen, two-parameter Curnier–Rakotomanana, one-parameter Curnier–Zysset, one-parameter Itskov, and two-parameter power and one- and two-parameter exponential Darijani–Naghdabadi strain tensor families (Doyle & Ericksen, 1956; Curnier & Rakotomanana, 1991; Itskov, 2004; Curnier & Zysset, 2006; Darijani, Naghdabadi, & Kargarnovin, 2010; Darijani & Naghdabadi, 2013). Korobeynikov (2019) himself introduce a new family of strain tensors – with symmetry in relation to the Logarithmic measure – which is also a subfamily of the Seth-Hill family. Beex (2019) created new strain measures that are fusions of the classical strain measures. Korobeynikov et al. (2022) developed explicit basis-free expressions for the Lagrangian fourth-order elasticity tensors for Hookean-type hyperelastic models and calibrated the material parameter of the strain measure family presented by Itskov (2004, 2019) to represent the experimentally obtained stress–strain relation for simple extension of a polyurethane material. Korobeynikov (2023) introduce a new family of Hookean-type isotropic hyperelastic material models which is associated with the classical family of strain tensors and is such that the rate counterparts of constitutive relations for material models from this family have a slightly modified form of constitutive relations for Hookean-type isotropic hypoelastic material models.

The broad set of studies that have as their theme the creation or study of strain measures, of which the articles highlighted above are part, aims to contribute to the modeling of the mechanical behavior of materials with application in engineering and bioengineering at large strains. In this context, current article presents the tensor format of a new family of strain measures based on the hyperbolic sine function: The Generalized Hyperbolic Sine (GHS) strain measure.

The Hookean-type constitutive models originated from the GHS family will be analyzed and compared with the models referring to the classical strain measures. For this purpose, the responses of the models to three pure modes of deformation will be studied: Simple Axial Extension (SAE), Equi-Biaxial Loading (E-BL) and Simple Shear (SS).

2 PROBLEM STATEMENT

Table 1 shows the Seth-Hill family of strain measures (also called classical strain measures) for the uniaxial case, all as a function of the stretching ratio (λ). The respective energetically conjugate stresses are also shown in the table, each one of them as a function of the 1D nominal stress (σ^N).

Table 1 Strain measures and conjugate stresses (1D).

Strain measure	Symbols		Strain (ϵ)	Stress (σ)
Green	ϵ^G	σ^G	$(\lambda^2 - 1)/2$	$\lambda^{-1}\sigma^N$
Biot	ϵ^B	σ^N	$\lambda - 1$	σ^N
Logarithmic	ϵ^L	σ^L	$\ln \lambda$	$\lambda \sigma^N$
Hyperbolic	ϵ^H	σ^H	$1 - \lambda^{-1}$	$\lambda^2 \sigma^N$
Almansi	ϵ^A	σ^A	$(1 - \lambda^{-2})/2$	$\lambda^3 \sigma^N$

The Seth-Hill family is expressed in a more concise manner by Equation (1),

$$g(\lambda) = \begin{cases} \frac{1}{m}(\lambda^m - 1) & m \neq 0 \\ \ln \lambda & m = 0 \end{cases} \quad \text{or} \quad \mathbf{G}(\mathbf{U}) = \begin{cases} \frac{1}{m}(\mathbf{U}^m - 1) & m \neq 0 \\ \ln \mathbf{U} & m = 0 \end{cases}, \quad (1)$$

where \mathbf{U} is the right stretch tensor. The variable m is an integer constant that can assume the following values: $m = -2$ (Almansi), -1 (Hyperbolic), 0 (Logarithmic), 1 (Biot) and 2 (Green). Constant m has the purpose of discriminating which strain measure of the Seth-Hill family is being analyzed/used. It should be noted here that, as this is a study of Hookean-type hyperelastic models, the choice of the strain measure also tries to describe the mechanical behavior of the material.

A challenge in the use of classical strain measures is that, for large strains, the Green and Biot are problematic in compression, as they do not tend to $-\infty$ when the stretching ratio approaches 0. In tension, Almansi and Hyperbolic do not present a monotonic increase with increasing stretching. The Logarithmic measure meets these two demands, however it shows a loss of stiffness along the entire tensile curve, a behavior uncommon among the materials used in engineering.

In this context, current article presents a family of strain measures based on a simple function, objective and versatile. With the presence of just one added non-zero real material constant, $n \in \mathbb{R}^*$, one can control the characteristics that are the main concern about the physical consistency of the strain measure: monotonic increase throughout the whole curve (first derivative always positive) and tendency to $-\infty$ when the stretch (λ) approaches 0. GHS strain measures family is given by

$$y(\lambda) = n^{-1} \sinh(n g(\lambda)) \quad n \neq 0 \quad \text{or} \quad \mathbf{Y}(\mathbf{U}) = n^{-1} \sinh(n \mathbf{G}(\mathbf{U})) \quad n \neq 0 \quad \text{GHS family} \quad (2)$$

where $g(\lambda)$ in Equation (2) is, *a priori*, any given strain measure. In this work, one restricts attention to when one has $g(\lambda)$ given by Equation (1),

$$y(\lambda) = \begin{cases} n^{-1} \sinh\left[\frac{n}{m}(\lambda^m - 1)\right] & m \neq 0 \\ n^{-1} \sinh(n \ln \lambda) = \frac{1}{2n}(\lambda^n - \lambda^{-n}) & m = 0 \end{cases} \quad \text{or} \quad \mathbf{Y}(\mathbf{U}) = \begin{cases} n^{-1} \sinh\left[\frac{n}{m}(\mathbf{U}^m - 1)\right] & m \neq 0 \\ \frac{1}{2n}(\mathbf{U}^n - \mathbf{U}^{-n}) & m = 0 \end{cases} \quad \text{GHS - Seth-Hill family} \quad (3)$$

Such concept, showed by Equation (3), is already present in the work of Greco and Peixoto (2021), but such article used only the Biot strain measure ($m = 0$) as an argument of the hyperbolic sine function and only covered uniaxial formulation. It is interesting to note that the strain family defined in Itskov (2004) is found to be a sub-family of the GHS – Seth-Hill family ($m = 0$).

Figure 1b, c, d, e f show, respectively, the sub-families derived from the use of: $m = 2$ (GHS-Green), $m = 1$ (GHS-Biot), $m = 0$ (GHS-Logarithmic), $m = -1$ (GHS-Hyperbolic) and $m = -2$ (GHS-Almansi). In the graphs, some values of n were used to exemplify some members of the new family, and for all graphs the value of $n = 0.1$ was presented to demonstrate the tendency to return to the original strain measure when n tends to zero. The subjective criterion used to choose the values of n was to select the ones which produced clearer and more illustrative graphs to show the versatility obtained by varying n . For each sub-family of strain measure, it was necessary to use different interval lengths to achieve this objective.

It is worth mentioning that, if necessary, the m values can vary beyond the limits $-2 < m < 2$ to better represent a given material. An important aspect that can be observed is that it is possible to cover a wide range of material behaviors: i) asymmetry between compression/tension, with greater stiffness in tension ($m > 1$); ii) symmetry between compression and tension ($m = 1$); and iii) asymmetry between compression/tension, with greater stiffness in compression ($m < 1$). At this point it can be established that with the variation of the variables m and n , several strain measures are obtained, and all these strain measures together form the GHS family, with each of these strain measures representing a hyperelastic model that, in turn, describes a certain material behavior.

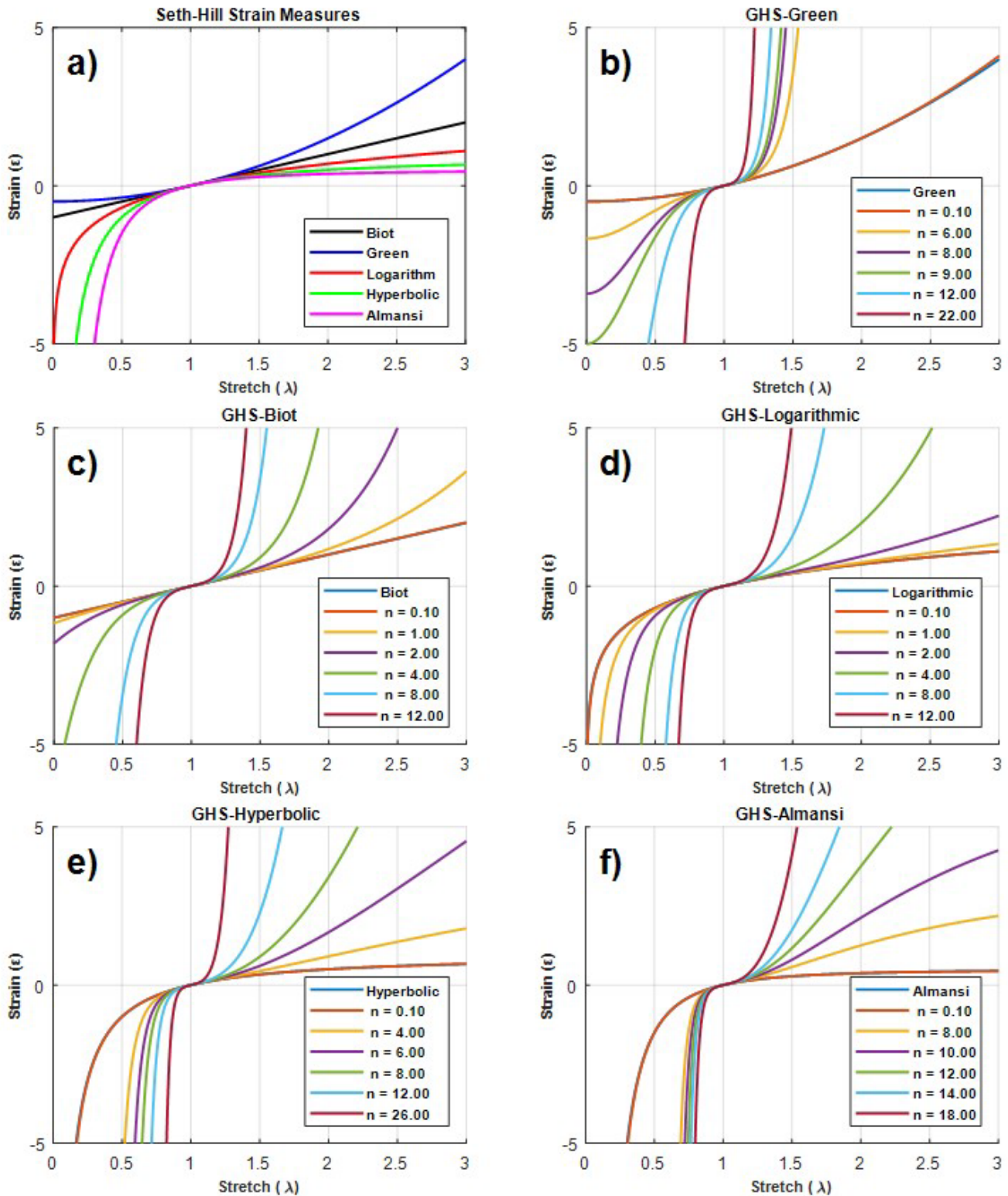


Figure 1 : Strain × stretch graph for: (a) Seth-Hill family; (b, c, d and e) GHS subfamilies with variation of n .

3 WORK-CONJUGATE STRESSES

Let $\boldsymbol{\varepsilon}^f = f(\lambda_i) (\boldsymbol{\alpha}_i \otimes \boldsymbol{\alpha}_i)$ and $\boldsymbol{\varepsilon}^k = k(\lambda_i) (\boldsymbol{\alpha}_i \otimes \boldsymbol{\alpha}_i)$ be arbitrary lagrangian strain tensors, where $\boldsymbol{\alpha}_i$ are the eigenvectors of \mathbf{U} . Further, let $\boldsymbol{\sigma}^f = \bar{\sigma}_{ij}^f (\boldsymbol{\alpha}_i \otimes \boldsymbol{\alpha}_j)$ and $\boldsymbol{\sigma}^k = \bar{\sigma}_{ij}^k (\boldsymbol{\alpha}_i \otimes \boldsymbol{\alpha}_j)$ be their work-conjugate stress tensors, respectively. Then, for the case of non-coalescent principal stretches, one writes according to Farahani and Naghdabadi (2003),

$$\begin{cases} \bar{\sigma}_{ii}^f = \frac{k'(\lambda_i)}{f'(\lambda_i)} \bar{\sigma}_{ii}^k & i = 1, 2, 3 \\ \bar{\sigma}_{ij}^f = \frac{k(\lambda_i) - k(\lambda_j)}{f(\lambda_i) - f(\lambda_j)} \bar{\sigma}_{ij}^k & i \neq j \end{cases} \quad (4)$$

If ϵ^k is the Green strain, Equation (4) becomes

$$\begin{cases} \bar{\sigma}_{ii}^f = \frac{\lambda_i}{f'(\lambda_i)} \bar{\sigma}_{ii}^G & i = 1, 2, 3 \\ \bar{\sigma}_{ij}^f = \frac{1}{2} \frac{\lambda_i^2 - \lambda_j^2}{f(\lambda_i) - f(\lambda_j)} \bar{\sigma}_{ij}^G & i \neq j \end{cases} \quad (5)$$

Equation (5) is fundamental for some algebraic manipulations in the next section. Particularly, the work-conjugate stress of the GHS – Seth-Hill strain family in Equation (3) is

$$m \neq 0 \begin{cases} \bar{\sigma}_{ii}^y = \lambda_i^{2-m} \operatorname{sech} \left[\frac{n}{m} (\lambda_i^m - 1) \right] \bar{\sigma}_{ii}^G & i = 1, 2, 3 \\ \bar{\sigma}_{ij}^y = \frac{n}{2} \frac{\lambda_i^2 - \lambda_j^2}{\sinh \left[\frac{n}{m} (\lambda_i^m - 1) \right] - \sinh \left[\frac{n}{m} (\lambda_j^m - 1) \right]} \bar{\sigma}_{ij}^G & i \neq j \end{cases} ; \quad m = 0 \begin{cases} \bar{\sigma}_{ii}^y = \frac{\lambda_i^2}{\cosh(n \ln \lambda_i)} \bar{\sigma}_{ii}^G & i = 1, 2, 3 \\ \bar{\sigma}_{ij}^y = \frac{n}{2} \frac{\lambda_i^2 - \lambda_j^2}{\sinh(n \ln \lambda_i) - \sinh(n \ln \lambda_j)} \bar{\sigma}_{ij}^G & i \neq j \end{cases} \quad (6)$$

Expressions of the Equations (4), (5) and (6) for the case of coalescent principal stretches are written easily following Farahani and Naghdabadi (2003), and are not given here.

4 PURE DEFORMATION MODES

This section presents the three pure deformation modes to be studied: SAE, E-BL in plane stress and SS in plane strain. Algebraic manipulations are performed to generate the equations analyzed through graph plotting in the Results section. Material is considered elastic, isotropic, and homogeneous.

4.1 Simple Axial Extension

The first deformation mode to be studied is the SAE. Here, it is considered that the deformation is produced by surface tractions (f) parallel to the X_1 axis, applied only on the faces of the prismatic body. Figure 2 shows a qualitative representation of the structure/loading system to be studied. It should be noted that the representation of applied forces is only illustrative and is intended to indicate the faces where loads are applied.

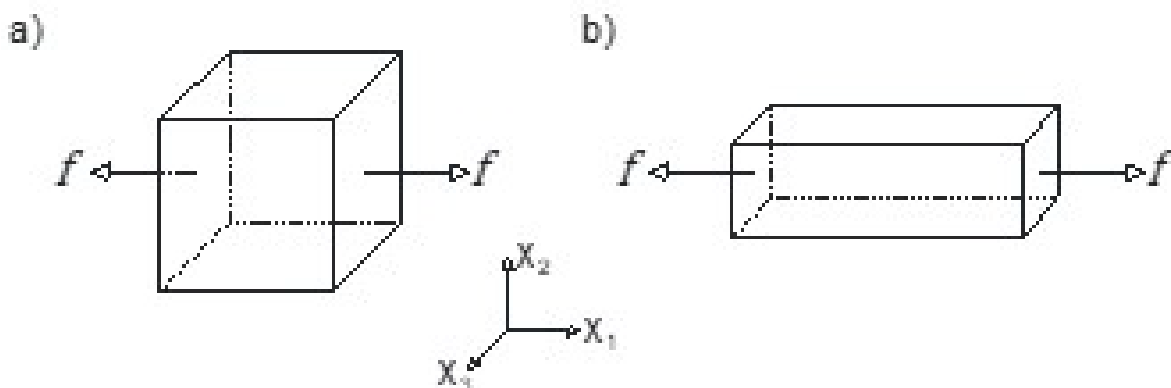


Figure 2: Simple Axial Extension: a) undeformed and b) deformed configurations.

The deformation gradient of the SAE is

$$[\mathbf{F}] = \begin{bmatrix} \lambda_1 & 0 & 0 \\ 0 & \lambda_2 & 0 \\ 0 & 0 & \lambda_3 \end{bmatrix}, \quad \text{with } \lambda_2 = \lambda_3. \quad (7)$$

Considering a generic work-conjugate pair of strain and stress ($\boldsymbol{\varepsilon}^f$ and $\boldsymbol{\sigma}^f$), the direct generalization of the classical Hooke's law for finite strains of isotropic materials together with the boundary conditions that characterize the SAE mode, through algebraic manipulations, leads to

$$\bar{\sigma}_{11}^f = z f(\lambda_1), \quad (8)$$

where the auxiliary variable z is

$$z = \frac{\mu(3\Lambda + 2\mu)}{\Lambda + \mu}. \quad (\Lambda \text{ and } \mu \text{ are the Lamé parameters}) \quad (9)$$

To compare the behavior of the Hookean-type constitutive models based on the classical strain measures and the GHS measure, it is necessary to substitute the strain measures and their respective conjugate stresses in Equation (8) and, finally, by means of relationships between the strain/stress measures, find the Nominal stress tensor \mathbf{P} (also known as the first Piola-Kirchhoff stress tensor). It is noteworthy that some authors (Marsden & Hughes, 1994; Ogden, 1997; Truesdell & Noll, 2004; Liu et al., 2014) name the Nominal stress tensor as the transposed tensor of \mathbf{P} , that is, \mathbf{P}^T , but for the SAE mode \mathbf{P}^T and \mathbf{P} coalesce, so this nomenclature issue is indifferent.

The strain measures to be studied are the ones from the Seth-Hill family in its lagrangean description and the GHS strain measure; Equations (1)₁ and (3)₁ show their 1D versions. Since $\mathbf{P} = \mathbf{F} \boldsymbol{\sigma}^G$, one concludes that $\sigma_{11}^G = P_{11}/\lambda_1$ for SAE. Substituting this expression in Equation (5), and using Equation (8), one has

$$P_{11} = z f(\lambda_1) f'(\lambda_1). \quad (10)$$

When working in a regime of large strains, the use of the Cauchy stress tensor $\boldsymbol{\sigma}^C$ is often advantageous compared to the Nominal stress tensor \mathbf{P} . With that in mind, the investigation of the behavior of the $\sigma_{11}^C \times \lambda_1$ relationship is as important as (or even more important than) the $P_{11} \times \lambda_1$. The passage from the Nominal stress tensor to Cauchy stress tensor is done through Equation (11) (Hackett, 2018) which becomes Equation (12) when the SAE mode conditions are considered. The variable J represents the determinant of \mathbf{F} .

$$[\boldsymbol{\sigma}^C] = J^{-1} [\mathbf{F}] [\mathbf{P}]^T. \quad (11)$$

$$\sigma_{11}^C = \frac{P_{11}}{\lambda_2^2}. \quad (12)$$

Next, since the definition of the Poisson's ratio is given by

$$\nu = -\frac{\varepsilon_{22}^f}{\varepsilon_{11}^f} = -\frac{\varepsilon_{33}^f}{\varepsilon_{11}^f}, \quad (13)$$

one can define the relationship between λ_1 and $\lambda_2 = \lambda_3$. Equation (14) (Korobeynikov, 2019) refers to the Seth-Hill strain measures with $m \neq 0$ and Equation (15) (Korobeynikov, 2019) refers to the Logarithmic strain measure ($m = 0$). The $\lambda_2 \times \lambda_1$ relationship for the GHS strain when $m \neq 0$ is given by the Equation (16) and when $m = 0$ by the Equation (17).

$$\lambda_2 = (1 + \nu - \nu \lambda_1^m)^{1/m}; \quad \text{Seth-Hill family (m} \neq 0) \tag{14}$$

$$\lambda_2 = \lambda_1^{-\nu}; \quad \text{Seth-Hill family (m} = 0) \tag{15}$$

$$\lambda_2 = \left\{ \frac{m}{n} \operatorname{arcsinh} \left\{ -\nu \sinh \left[\frac{n}{m} (\lambda_1^m - 1) \right] \right\} + 1 \right\}^{1/m}; \quad \text{GHS – Seth-Hill family (m} \neq 0) \tag{16}$$

$$\lambda_2 = \exp \left\{ n^{-1} \operatorname{arcsinh} \left[-\nu \sinh (n \ln \lambda_1) \right] \right\}. \quad \text{GHS – Seth-Hill family (m} = 0) \tag{17}$$

Substituting Equation (10) in Equation (12), and using Equations (14) to (17), one finds the following $\sigma_{11}^c \times \lambda_1$ relationships to be used for SAE:

$$\sigma_{11}^c = \frac{z}{m} \lambda_1^{m-1} (\lambda_1^m - 1) (1 + \nu - \nu \lambda_1^m)^{-2/m}, \quad \text{Seth-Hill family (m} \neq 0) \tag{18}$$

$$\sigma_{11}^c = z \lambda_1^{2\nu-1} \ln \lambda_1, \quad \text{Seth-Hill family (m} = 0) \tag{19}$$

$$\sigma_{11}^c = \frac{z \lambda_1^{m-1}}{n} \cosh \left[\frac{n}{m} (\lambda_1^m - 1) \right] \sinh \left[\frac{n}{m} (\lambda_1^m - 1) \right] \left\{ \frac{m}{n} \operatorname{arcsinh} \left\{ -\nu \sinh \left[\frac{n}{m} (\lambda_1^m - 1) \right] \right\} + 1 \right\}^{-2/m}, \quad \text{GHS – Seth-Hill family (m} \neq 0) \tag{20}$$

$$\sigma_{11}^c = \frac{z}{n \lambda_1} \sinh (n \ln \lambda_1) \cosh (n \ln \lambda_1) \exp \left\{ -2n^{-1} \operatorname{arcsinh} \left[-\nu \sinh (n \ln \lambda_1) \right] \right\}. \quad \text{GHS – Seth-Hill family (m} = 0) \tag{21}$$

4.2 Equi-Biaxial Loading

The pure mode generated by an E-BL, represented by Figure 3, consists of applying equal axial loads in two principal directions of a cubic solid. The forces represented in Figure 3 are merely illustrative and serve only to identify the faces on which the loads are applied. It is a deformation mode closely associated with the study of membranes made of elastic materials capable of withstanding large deformations, with polymers, elastomers and soft biological tissues being relevant examples.

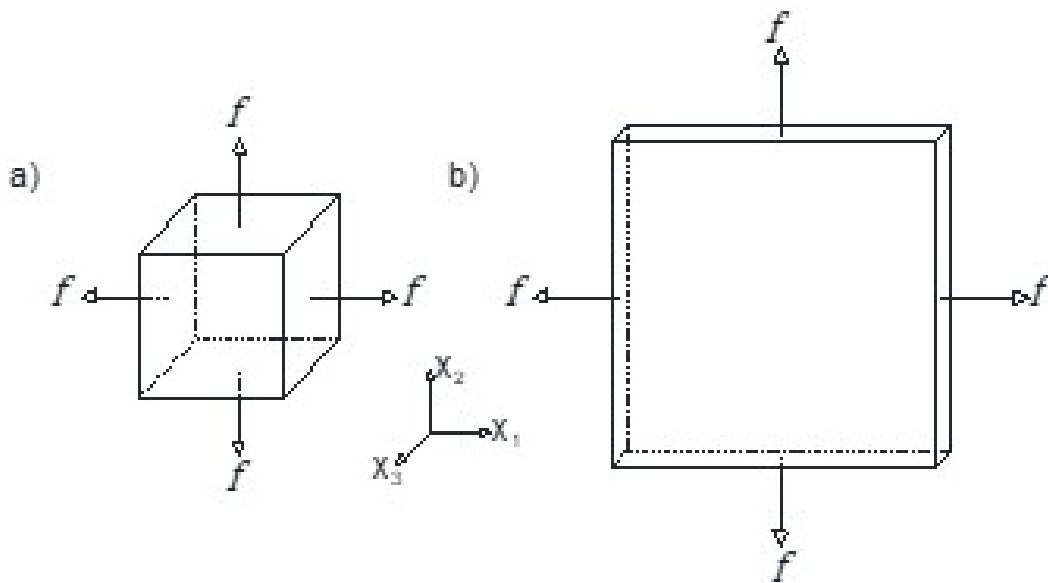


Figure 3: Equi-Biaxial loading: a) undeformed and b) deformed configurations.

The development of the formulation is very similar to the one performed for the SAE mode. The deformation gradient of the E-BL, represented by the Equation (22), with the boundary conditions that characterize the E-BL lead to new relationships between the principal stretches and to a different expression for the auxiliary variable z :

$$[\mathbf{F}] = \begin{bmatrix} \lambda_1 & 0 & 0 \\ 0 & \lambda_2 & 0 \\ 0 & 0 & \lambda_3 \end{bmatrix}, \quad \text{with } \lambda_1 = \lambda_2, \quad (22)$$

$$z = \frac{2\mu(3\Lambda + 2\mu)}{\Lambda + 2\mu}. \quad (23)$$

It becomes clear now how opportune it is to use of the auxiliary variable z as one notice that Equation (8), defined for the SAE mode, can be reused here in E-BL mode. The passage from P_{11} to σ_{11}^c is also done using Equation (11), but for E-BL mode the conditions change to $\lambda_1 = \lambda_2 \neq \lambda_3$. Therefore, σ_{11}^c is now expressed by

$$\sigma_{11}^c = \frac{P_{11}}{\lambda_1 \lambda_3}. \quad (24)$$

Hooke's law together with the conditions for the E-BL pure mode result in a new expression for the Poisson's ratio:

$$\nu = \frac{\varepsilon_{33}^f}{-2\varepsilon_{11}^f + \varepsilon_{33}^f} = \frac{\varepsilon_{33}^f}{-2\varepsilon_{22}^f + \varepsilon_{33}^f}. \quad (25)$$

Using the new definition for the Poisson's ratio it is possible to find the expressions for the $\lambda_3 \times \lambda_1$ relationship:

$$\lambda_3 = \left[\frac{\nu(1 - 2\lambda_1^m) + 1}{1 - \nu} \right]^{1/m}, \quad \text{Seth-Hill family (m} \neq 0) \quad (26)$$

$$\lambda_3 = \lambda_1^{2\nu/(\nu-1)}, \quad \text{Seth-Hill family (m} = 0) \quad (27)$$

$$\lambda_3 = \left\{ \frac{m}{n} \operatorname{arcsinh} \left\{ \frac{2\nu}{\nu-1} \sinh \left[\frac{n}{m} (\lambda_1^m - 1) \right] \right\} + 1 \right\}^{1/m}, \quad \text{GHS - Seth-Hill family (m} \neq 0) \quad (28)$$

$$\lambda_3 = \exp \left\{ n^{-1} \operatorname{arcsinh} \left[\frac{2\nu}{\nu-1} \sinh(n \ln \lambda_1) \right] \right\}. \quad \text{GHS - Seth-Hill family (m} = 0) \quad (29)$$

and, finally, the expressions for the axial component of the Cauchy stress are found:

$$\sigma_{11}^c = \frac{z}{m} \lambda_1^{m-2} (\lambda_1^m - 1) \left(\frac{-2\nu\lambda_1^m + \nu + 1}{1 - \nu} \right)^{-1/m}, \quad \text{Seth-Hill family (m} \neq 0) \quad (30)$$

$$\sigma_{11}^c = z \lambda_1^{2(1-2\nu)/(\nu-1)} \ln \lambda_1, \quad \text{Seth-Hill family (m} = 0) \quad (31)$$

$$\sigma_{11}^c = \frac{z \lambda_1^{m-2}}{n} \cosh \left[\frac{n}{m} (\lambda_1^m - 1) \right] \sinh \left[\frac{n}{m} (\lambda_1^m - 1) \right] \left\{ \frac{m}{n} \operatorname{arcsinh} \left\{ \frac{2\nu}{\nu-1} \sinh \left[\frac{n}{m} (\lambda_1^m - 1) \right] \right\} + 1 \right\}^{-1/m}, \quad \text{GHS - Seth-Hill (m} \neq 0) \quad (32)$$

$$\sigma_{ii}^c = \frac{z}{n\lambda_1^2} \sinh(n \ln \lambda_1) \cosh(n \ln \lambda_1) \exp\left\{-n^{-1} \operatorname{arcsinh}\left[\frac{2\nu}{\nu-1} \sinh(n \ln \lambda_1)\right]\right\}. \quad \text{GHS – Seth-Hill family (m = 0)} \quad (33)$$

4.3 Simple shear

The SS mode (Figure 4) is of theoretical interest for the study of the behavior of different constitutive models when forces generate rotations.

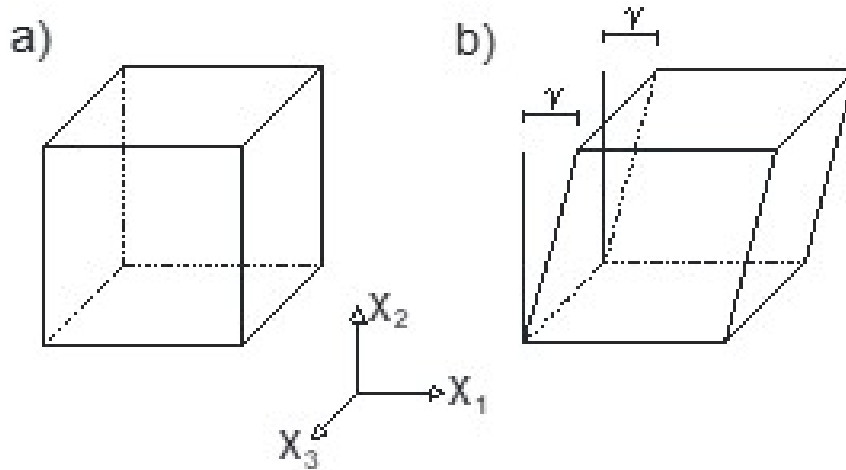


Figure 4: Simple shear: a) undeformed and b) deformed configuration.

The deformation gradient of the SS mode is:

$$[\mathbf{F}] = \begin{bmatrix} 1 & \gamma & 0 \\ 0 & 1 & 0 \\ 0 & 0 & 1 \end{bmatrix}. \quad (34)$$

By introducing an angle β , defined by

$$\beta = \operatorname{arctg}\left(\frac{\gamma}{2}\right), \quad \text{with} \quad 0 \leq \beta \leq \frac{\pi}{2}, \quad (35)$$

Hashiguchi and Yamakawa (2012) have defined the key mathematical expressions which define the SS mode:

$$\lambda_1 = \frac{1 + \sin \beta}{\cos \beta}, \quad \lambda_2 = \frac{1 - \sin \beta}{\cos \beta}, \quad \lambda_3 = 1, \quad [\mathbf{U}] = \begin{bmatrix} \cos \beta & \sin \beta & 0 \\ \sin \beta & \frac{1 + \sin^2 \beta}{\cos \beta} & 0 \\ 0 & 0 & 1 \end{bmatrix}, \quad (36)$$

$$[\mathbf{R}] = \begin{bmatrix} \cos \beta & \sin \beta & 0 \\ -\sin \beta & \cos \beta & 0 \\ 0 & 0 & 1 \end{bmatrix} \quad \text{and} \quad [{}^v\mathbf{Q}] = \begin{bmatrix} \frac{\cos \beta}{\sqrt{2 + 2 \sin \beta}} & \frac{\cos \beta}{\sqrt{2 - 2 \sin \beta}} & 0 \\ \frac{\sin \beta + 1}{\sqrt{2 + 2 \sin \beta}} & \frac{\sin \beta - 1}{\sqrt{2 - 2 \sin \beta}} & 0 \\ 0 & 0 & 1 \end{bmatrix}. \quad (37)$$

Using Hooke's Law and performing pertinent algebraic manipulations, one reaches the mathematical expression that defines the $\sigma_{12}^c \times \gamma$ relationship for the Seth-Hill family with $m \neq 0$,

$$\sigma_{12}^c = \frac{\lambda_1^{m-1}}{2m\lambda_1} [\cos \beta + \gamma(1 + \sin \beta)] [2\mu(\lambda_1^m - 1) + \Lambda(\lambda_1^m + \lambda_2^m - 2)] - \frac{\lambda_2^{m-1}}{2m\lambda_2} [\cos \beta + \gamma(\sin \beta - 1)] [2\mu(\lambda_2^m - 1) + \Lambda(\lambda_1^m + \lambda_2^m - 2)]. \quad (38)$$

For the Seth-Hill family with $m = 0$ one has

$$\sigma_{12}^c = \frac{1}{2\lambda_1^2} [\cos \beta + \gamma(1 + \sin \beta)] [2\mu \ln \lambda_1 + \Lambda(\ln \lambda_1 + \ln \lambda_2)] - \frac{1}{2\lambda_2^2} [\cos \beta + \gamma(\sin \beta - 1)] [2\mu \ln \lambda_2 + \Lambda(\ln \lambda_1 + \ln \lambda_2)]. \quad (39)$$

For GHS – Seth-Hill family with $m \neq 0$ one obtains

$$\begin{aligned} \sigma_{12}^c &= \frac{\lambda_1^{m-2}}{2n} \cosh \left[\frac{n}{m} (\lambda_1^m - 1) \right] [\cos \beta + \gamma(1 + \sin \beta)] \left\{ 2\mu \sinh \left[\frac{n}{m} (\lambda_1^m - 1) \right] + \Lambda \left\{ \sinh \left[\frac{n}{m} (\lambda_1^m - 1) \right] + \sinh \left[\frac{n}{m} (\lambda_2^m - 1) \right] \right\} \right\} + \\ &- \frac{\lambda_2^{m-2}}{2n} \cosh \left[\frac{n}{m} (\lambda_2^m - 1) \right] [\cos \beta + \gamma(\sin \beta - 1)] \left\{ 2\mu \sinh \left[\frac{n}{m} (\lambda_2^m - 1) \right] + \Lambda \left\{ \sinh \left[\frac{n}{m} (\lambda_1^m - 1) \right] + \sinh \left[\frac{n}{m} (\lambda_2^m - 1) \right] \right\} \right\}. \end{aligned} \quad (40)$$

And, finally, for the GHS – Seth-Hill family with $m = 0$ one reaches

$$\begin{aligned} \sigma_{12}^c &= \frac{\cosh(n \ln \lambda_1)}{2n\lambda_1^2} [\cos \beta + \gamma(1 + \sin \beta)] \left\{ 2\mu \sinh(n \ln \lambda_1) + \Lambda \left\{ \sinh(n \ln \lambda_1) + \sinh(n \ln \lambda_2) \right\} \right\} + \\ &- \frac{\cosh(n \ln \lambda_2)}{2n\lambda_2^2} [\cos \beta + \gamma(\sin \beta - 1)] \left\{ 2\mu \sinh(n \ln \lambda_2) + \Lambda \left\{ \sinh(n \ln \lambda_1) + \sinh(n \ln \lambda_2) \right\} \right\}. \end{aligned} \quad (41)$$

5 RESULTS AND DISCUSSIONS

With the mathematical expressions previously defined in section 4, graphs are plotted to analyze the physical coherence of the responses obtained. The results were obtained using a Poisson's ratio referring to an approximately incompressible material ($0.47 < \nu < 0.50$), but proposed methodology is not restricted for incompressible material modeling.

To build an analysis regarding the capacity of the constitutive models studied to generate physically coherent responses, as well as to identify the limits of this capacity, some criteria are presented below. Criterion I and II are analogous to the criterion presented by Hill (1968) in which the need to have a smooth monotone function was established. Criterion III was originally presented by Treloar (1975). Criterion IV is inspired by discussions done by Batra (1998) and Batra (2001).

- **Criterion I:** the greater the axial tensile force/stress in the X_1 direction (the greater σ_{11}^c), the greater the stretch in the X_1 direction (greater λ_1);
- **Criterion II:** the greater the axial compressive force/stress in the X_1 direction (the smaller σ_{11}^c), the smaller the stretch in the X_1 direction (smaller λ_1);
- **Criterion III:** on the $\sigma_{11}^c \times \lambda_1$ graphs, it is expected that in compression, as the value of λ_1 tends to 0, the axial component of stress (σ_{11}^c) tends to minus infinity, because otherwise it is common to face problems of convergence and computational instability in simulations, as stated by Beex (2019), in addition to meaning that a finite value of stress compression would make the material disappear. When criterion II is not met for $\sigma_{11}^c \times \lambda_1$ graphs, criterion III is not met either;

- Criterion IV:** some constitutive models have stretches limits that are different from 0 or infinity, but without loss of physical coherence. It is verified that for a finite stretch value, different from 0 or infinity, the force/stress value tends to infinity, that is, there is a vertical asymptote in this stretch value. This criterion concerns the limitation of the range of representation capacity of a given constitutive model, being related to its suitability in the modeling of a given material, and not to the occurrence of physical inconsistency.

5.1 Simple Axial Extension results

To represent rubber-like materials it is used a value of $E = 4$ [MPa] for the Young’s modulus and a Poisson’s ratio of $\nu = 0.48$. Firstly, the $\sigma_{11}^C \times \lambda_1$ relationship is examined for the SAE mode.

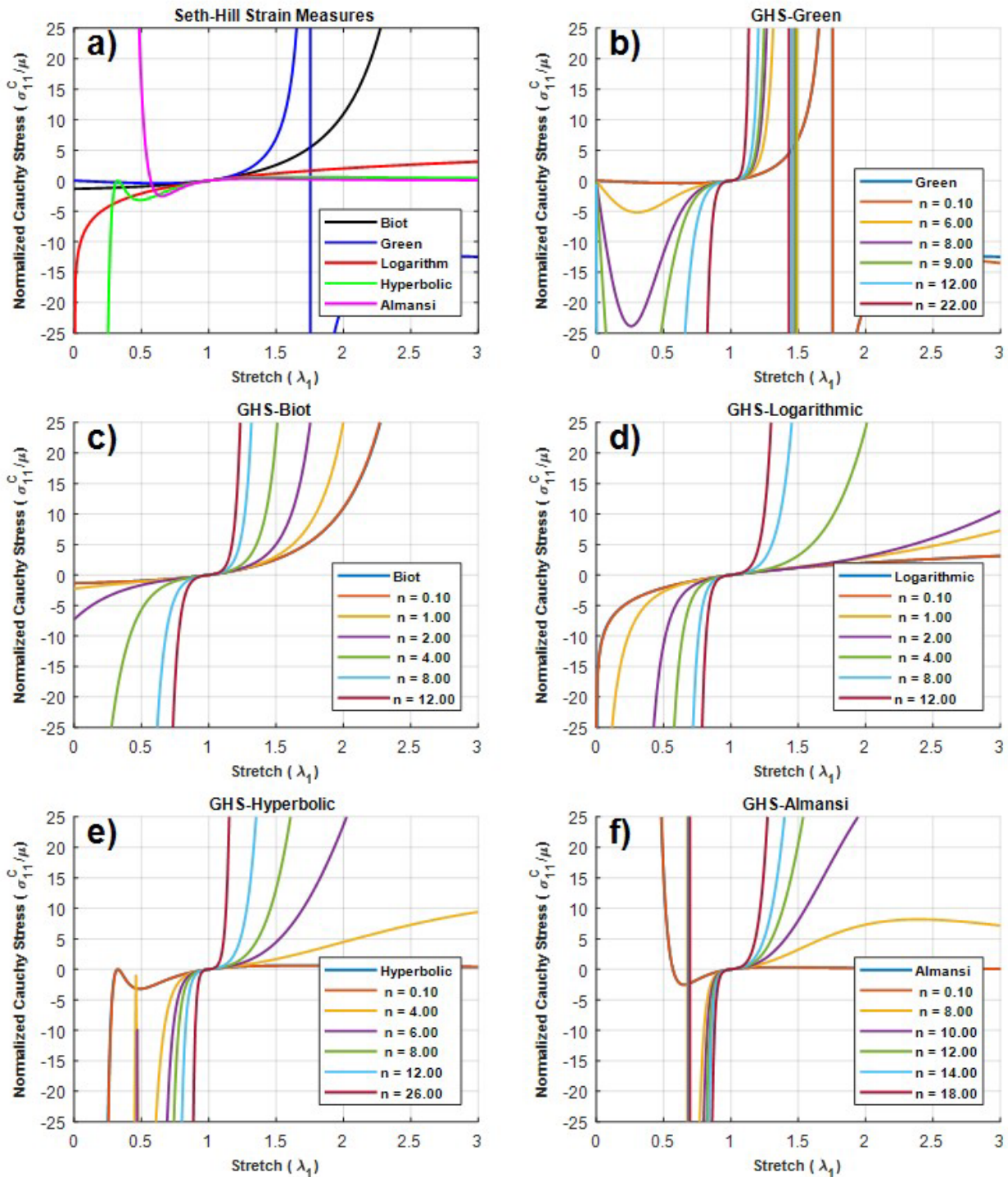


Figure 5: Simple Uniaxial Extension: $\sigma_{11}^C \times \lambda_1$ graph for (a) Seth-Hill family; (b, c, d and e) GHS subfamilies with variation of n .

Figure 5 shows the $\sigma_{11}^f \times \lambda_1$ graphs for the SAE mode, with: a) representing the Seth-Hill family, b) the GHS – Green family, c) the GHS – Biot family, d) the GHS – Logarithmic family, e) the GHS – Green family and f) the GHS – Green family.

To better understand the physical meaning of the material parameter n , one can analyze the graphs from Figure 5b, c, d, e, and f, each one showing the strain measures of one of the GHS subfamilies for different values of the n parameter. In the compression part of the curve, starting from $\lambda = 1$, as one moves to the left ($\lambda < 1$), the greater the value of n , the greater the tangent stiffness (first derivative) value and the greater the rate of increase of the tangent stiffness (second derivative, negative for compression). In the tension part of the curve, starting from $\lambda = 1$, as one moves to the right ($\lambda > 1$), the greater the value of n , the greater the tangent stiffness value (first derivative) and the greater the rate of increase of the stiffness tangent (second derivative). Thus, it can be said that the parameter n controls the rate of increase of the tangent stiffness, both in compression and tension.

Now one begins the analysis of the physical coherence limitations by the Seth-Hill family (Figure 5a). The Logarithmic strain model does show a monotonic increase in stress as the stretching ratio increases, so it meets criteria I and II, furthermore, the stress axial component tends to $-\infty$ when λ_3 tends to 0, so it also meets criterion III. The curves referring to the Hyperbolic and Almansi measures fail to meet criterion II at points $\lambda_1 \approx 0.48$ and $\lambda_1 \approx 0.65$, respectively, and criterion I at $\lambda_1 \approx 1.66$ and $\lambda_1 \approx 1.33$, respectively. The Green model does not have physical coherence in compression (II) below $\lambda_1 \approx 0.63$. In tension, the Green and Biot models meet criterion I, as they do not lose physical coherence, however these curves have vertical asymptotes (IV) in $\lambda_1 \approx 1.76$ and $\lambda_1 \approx 3.1$, respectively, meaning that materials that are capable of being subjected to stretches greater than these values through the imposition of finite loads cannot be represented by these models. In compression, Biot meets criteria II but not III. Figure 6 resume the interval of physical coherence for the Seth-Hill strain measures.

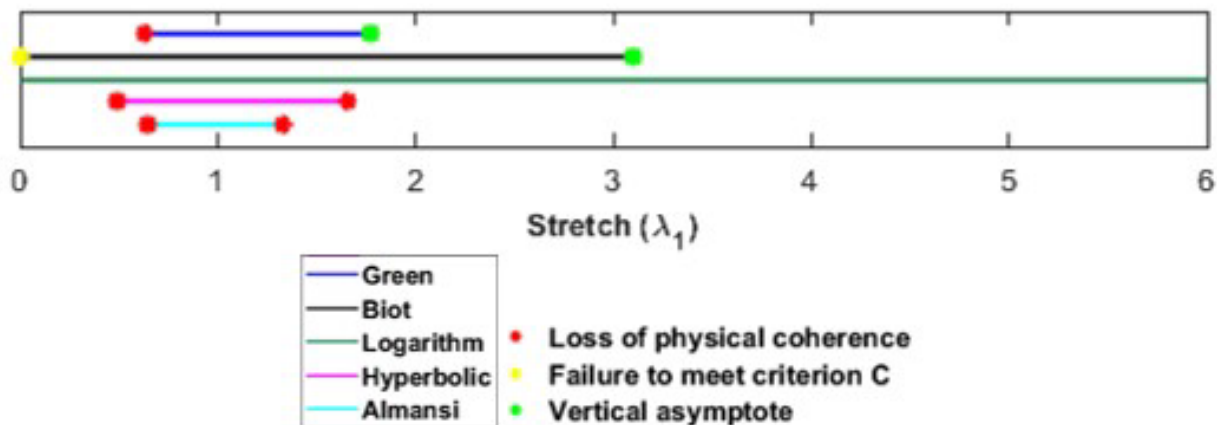


Figure 6: Summary of the Seth-Hill family limitations for SAE.

In addition to the objective/quantitative analysis, some subjective/qualitative observations regarding the behavior of constitutive models are worth mentioning. Even though the Logarithmic model has a monotonic increase in tension as strain increases, it also shows a continuous decrease in stiffness, which is not negative, but decreases sharply and continuously, which characterizes an unusual behavior for materials that support large deformations.

Looking at Figure 5a, b, c, d and e, some general observations can be made about the behavior of the GHS family of strain measures. As the value of n tends to zero the GHS strain measure tends to recover the behavior of the original strain measure, that is why all the graphs have the $n = 0.1$ presented, to show that property of the GHS family. Given the nature of the hyperbolic sine function, its use improves all the criteria regarding the physical consistency: I, II and III. About the criteria IV, one notes that the variation of n can vary the value of λ_1 where the asymptote occurs, which is useful in the representation of different materials. The great variety of curves originated have the capacity to represent a great variety of materials, for materials with a greater stiffness in compression than in tension, for example, one can search within the sub-family with $m \leq 0$ (Logarithmic, Hyperbolic and Almansi), and when the material behavior goes the other way around, with a higher stiffness in tension than in compression, the use of the sub-family with $m > 0$ is more appropriate. One remembers that values of m outside $-2 \leq m \leq 2$ are valid, as also the use of the hyperbolic sine function in other strain measures

outside the Seth-Hill family. Regarding the qualitative poor behavior of the Logarithmic strain measure in tension, the variation of n clearly improves it.

5.2 Equi-biaxial Loading results

The same material parameters used in the study of the SAE mode will be used here in the analysis of the E-BL mode, as well as the same stretch interval. Criteria I, II, III and IV will also be repeated here, as they were designed to make sense for both deformation modes. Figure 7 presents the results for the E-BL mode, with the format and order used in Figure 5.

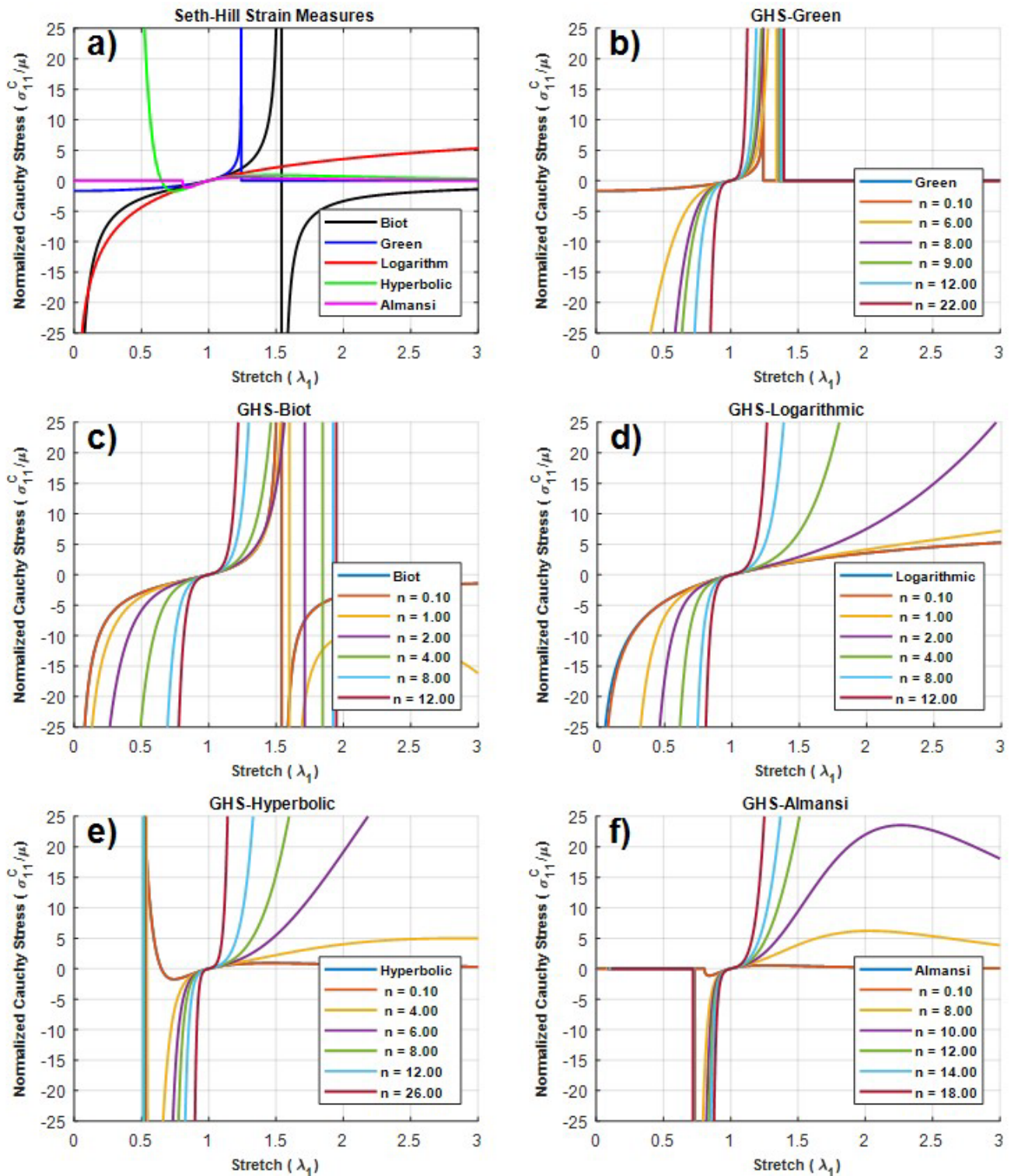


Figure 7: EquiBiaxial Loading: $\sigma_{11}^c \times \lambda_1$ graph for (a) Seth-Hill family; (b, c, d and e) GHS subfamilies with variation of n .

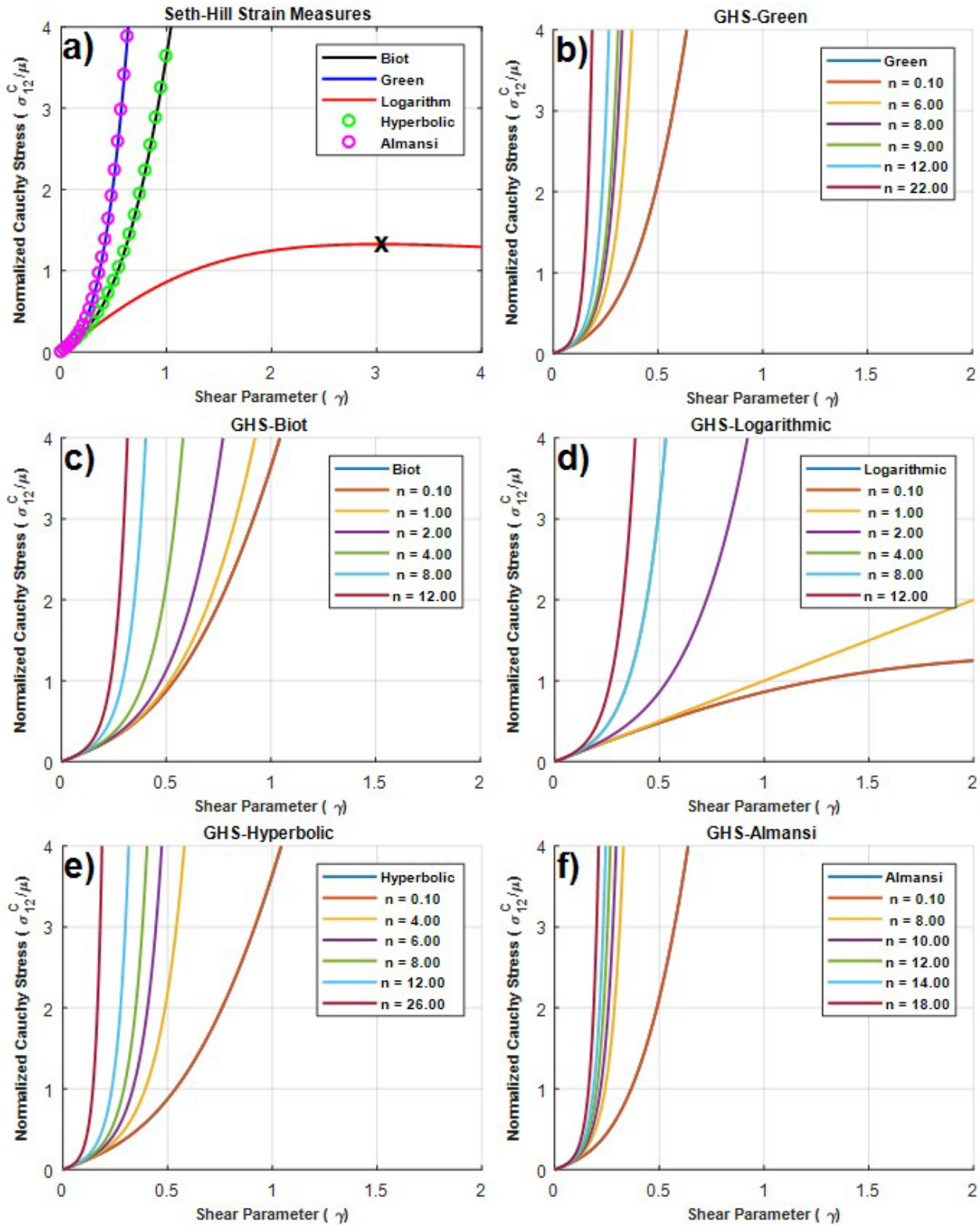


Figure 9: Simple Shear $\sigma_{12}^c \times \gamma$ graph for (a) Seth-Hill family; (b, c, d and e) GHS subfamilies with variation of n .

6 CONCLUSION

This article has presented the Generalized Hyperbolic Sine (GHS) strain measures family in its tensor form. A broad analytical study was carried to compare the behavior of the classical (Seth-Hill family) strain measures and the GHS family through the analysis of the responses of their Hookean-type constitutive models for three pure strain modes: SAE, E-BL

and SS. For SAE and E-BL modes, new generic mathematical expressions that relates the axial component of the Cauchy stress to the parallel stretching ratio ($\sigma_{11}^c \times \lambda_1$), suitable to any given strain measure function, were presented and applied for the GHS family of strain measures.

Graphical responses of the GHS and Seth-Hill families, concerning the studied pure modes of deformation, were analyzed using four established criteria from relevant literature to assess the physical coherence intervals of their Hookean-type hyperelastic models. The GHS family, which uses a simple normalized form of the hyperbolic sine function, proved itself capable of overcoming the main drawbacks of the classical strain measures, enhancing the physical behavior of the Seth-Hill strain measures, and providing versatility with the addition of just one material constant, n . An important feature is the clear physical meaning of n : control, both in tension and compression, the rate of increase of the stiffness as the force/stress increases.

This study only considered isotropic, homogeneous and hyperelastic material behavior, and was limited to the analytical study of three isolated pure deformation modes. Even though, *a priori*, any strain measure can be used as the argument for the proposed normalized hyperbolic sine function (Equation 2), only the Seth-Hill family of strain measures were investigated. For future research that continue the subject, one may add physical nonlinear phenomena to the Hookean-type hyperelastic models, such as: plasticity, damage mechanics and creep phenomena. Furthermore, the use of the GHS Hookean-type hyperelastic models to represent experimental data obtained for pure deformation modes and its implementation in Finite Element Method software seem like natural next steps for this article too. This article used quasi-incompressible material parameter in the analytical investigation, but the formulation presented can also be applied to compressible materials, so the potential of exploring GHS Hookean-type hyperelastic models for modeling compressible materials warrants further investigation.

Within the path of modeling hyperelastic materials in which direct generalization of the classical Hooke's law for finite strains is used, this work contributes by presenting the simple, objective, and versatile GHS family of strain measures, with good quantitative and qualitative responses.

ACKNOWLEDGMENTS

The authors thank Fundação de Amparo à Pesquisa do Estado de Minas Gerais (FAPEMIG), Conselho Nacional de Desenvolvimento Científico e Tecnológico (CNPq) and Coordenação de Aperfeiçoamento de Pessoal de Nível Superior (CAPES) for their research financial supports.

Author's Contributions: Conceptualization, M Greco and DHN Peixoto; Methodology, DHN Peixoto and DB Vasconcellos; Investigation, DHN Peixoto and DB Vasconcellos; Writing - original draft, DHN Peixoto; Writing - review & editing, DHN Peixoto, DB Vasconcellos and M Greco; Supervision, M Greco.

Editor: Rogério José Marczak

References

- Batra, R. C. (1998). Linear Constitutive Relations in Isotropic Finite Elasticity. *Journal of Elasticity*, 51, 243–245.
- Batra, R. C. (2001). Comparison of results from four linear constitutive relations in isotropic finite elasticity. *International Journal of Non-Linear Mechanics*, 36, 421–432.
- Beex, L. A. A. (2019). Fusing the Seth–Hill strain tensors to fit compressible elastic material responses in the nonlinear regime. *International Journal of Mechanical Sciences*, 163, 105072.
- Cao, J., Ding, X.-F., Yin, Z.-N., & Xiao, H. (2017). Large elastic deformations of soft solids up to failure: new hyperelastic models with error estimation. *Acta Mechanica*, 228, 1165–1175.
- Chagnon, G., Rebouah, M., & Favier, D. (2015). Hyperelastic Energy Densities for Soft Biological Tissues: A Review. *Journal of Elasticity*, 120, 129–160.
- Curnier, A., & Rakotomanana, L. (1991). Generalized Strain and Stress Measures: Critical Survey and New Results. *Engineering Transactions*, 39, 461–538.

- Curnier, A., & Zysset, Ph. (2006). A family of metric strains and conjugate stresses, prolonging usual material laws from small to large transformations. *International Journal of Solids and Structures*, 43, 3057–3086.
- Darijani, H., & Naghdabadi, R. (2013). Kinematics and kinetics modeling of thermoelastic continua based on the multiplicative decomposition of the deformation gradient. *International Journal of Engineering Science*, 62, 56–69.
- Darijani, H., Naghdabadi, R., & Kargarnovin, M. H. (2010). Hyperelastic materials modelling using a strain measure consistent with the strain energy postulates. *Proceedings of the Institution of Mechanical Engineers, Part C: Journal of Mechanical Engineering Science*, 224, 591–602.
- Doyle, T. C., & Ericksen, J. L. (1956). *nonlinear elasticity*. Academic Press.
- Farahani, K., & Bahai, H. (2004). Hyper-elastic constitutive equations of conjugate stresses and strain tensors for the Seth–Hill strain measures. *International Journal of Engineering Science*, 42, 29–41.
- Farahani, K., & Naghdabadi, R. (2003). Basis free relations for the conjugate stresses of the strains based on the right stretch tensor. *International Journal of Solids and Structures*, 40, 5887–5900.
- Firouzi, N., & Amabili, M. (2024). Two-dimensional growth of incompressible and compressible soft biological tissues. *European Journal of Mechanics - A/Solids*, 103, 105150.
- Greco, M., & Peixoto, D. H. N. (2021). Comparative assessments of strain measures for nonlinear analysis of truss structures at large deformations. *Engineering Computations*, 39, 1621–1641.
- Hackett, R. M. (2018). *Hyperelasticity Primer* (2nd ed. edição.). Cham: Springer.
- Hashiguchi, K., & Yamakawa, Y. (2012). *Introduction to Finite Strain Theory for Continuum Elasto-Plasticity* (1st edition.). Chichester West Sussex: Wiley.
- Hill, R. (1968). On constitutive inequalities for simple materials—I. *Journal of the Mechanics and Physics of Solids*, 16, 229–242.
- Hill, Rodney. (1979). Aspects of Invariance in Solid Mechanics. In C.-S. Yih (Ed.), *Advances in Applied Mechanics* (Vol. 18, pp. 1–75). Elsevier.
- Itskov, M. (2004). On the application of the additive decomposition of generalized strain measures in large strain plasticity. *Mechanics Research Communications*, 31, 507–517.
- Itskov, M. (2019). *Tensor Algebra and Tensor Analysis for Engineers: With Applications to Continuum Mechanics* (5th ed. 2019 edition.). New York, NY: Springer.
- Kang, J., Tan, L.-X., Liu, Q.-P., Wang, S.-Y., Bruhns, O. T., & Xiao, H. (2023). Unified and accurate simulation for large elastic strain responses of rubberlike soft materials under multiple modes of loading. *Continuum Mechanics and Thermodynamics*.
- Korobeynikov, S. N. (2019). Objective Symmetrically Physical Strain Tensors, Conjugate Stress Tensors, and Hill’s Linear Isotropic Hyperelastic Material Models. *Journal of Elasticity*, 136, 159–187.
- Korobeynikov, S. N. (2023). Families of Hooke-like isotropic hyperelastic material models and their rate formulations. *Archive of Applied Mechanics*, 93, 3863–3893.
- Korobeynikov, S. N., Larichkin, A. Yu., & Rotanova, T. A. (2022). Hyperelasticity models extending Hooke’s law from small to moderate strains and experimental verification of their scope of application. *International Journal of Solids and Structures*, 252, 111815.
- Kossa, A., Valentine, M. T., & McMeeking, R. M. (2023). Analysis of the compressible, isotropic, neo-Hookean hyperelastic model. *Meccanica*, 58, 217–232.
- Liu, W. K., Moran, B., Belytschko, T., & Elkhodary, K. (2014). *Nonlinear Finite Elements for Continua and Structures* (2nd edition.). Chichester, West Sussex, United Kingdom: Wiley.
- Mansouri, M. R., Darijani, H., & Baghani, M. (2017). On the Correlation of FEM and Experiments for Hyperelastic Elastomers. *Experimental Mechanics*, 57, 195–206.
- Marsden, J. E., & Hughes, T. J. R. (1994). *Mathematical Foundations of Elasticity* (Revised ed. edition.). New York: Dover Publications.

- Melly, S. K., Liu, L., Liu, Y., & Leng, J. (2022). A phenomenological constitutive model for predicting both the moderate and large deformation behavior of elastomeric materials. *Mechanics of Materials*, 165, 104179.
- Mihai, L. A., & Goriely, A. (2017). How to characterize a nonlinear elastic material? A review on nonlinear constitutive parameters in isotropic finite elasticity. *Proceedings of the Royal Society A: Mathematical, Physical and Engineering Sciences*, 473, 20170607.
- Ogden, R. W. (1997). *Non-Linear Elastic Deformations (Reprint edition.)*. Mineola, NY: Dover Publications.
- Park, J., Kim, C., & Lee, H. (2023). Prediction of Nonlinear Stress-strain Behaviors with Artificial Neural Networks and Its Application for Automotive Rubber Parts. *International Journal of Automotive Technology*, 24, 1481–1491.
- Peirlinck, M., Linka, K., Hurtado, J. A., & Kuhl, E. (2024). On automated model discovery and a universal material subroutine for hyperelastic materials. *Computer Methods in Applied Mechanics and Engineering*, 418, 116534.
- Saucedo-Mora, L., García-Bañales, O., Montáns, F.J., & Benítez, J.M. (2021). A two-parameter strain energy function for brain matter: An extension of the Hencky model to incorporate locking. *Brain Multiphysics* 2.
- Seth, B. R. (1961). *Generalized strain measure with applications to physical problems*. Wisconsin Univ-Madison Mathematics Research Center.
- Stumpf, F. T., & Marczak, R. J. (2021). Constitutive framework of a new hyperelastic model for isotropic rubber-like materials for finite element implementation. *Latin American Journal of Solids and Structures*, 18, e346.
- Treloar, L. R. G. (1975). *The Physics of Rubber Elasticity*. OUP Oxford.
- Truesdell, C., & Noll, W. (2004). *The Non-Linear Field Theories of Mechanics*. Springer Science & Business Media.
- Xiao, H., & Chen, L. S. (2002). Hencky's elasticity model and linear stress-strain relations in isotropic finite hyperelasticity. *Acta Mechanica*, 157, 51–60.